EFFECTS OF CENTERBODY ON THE VORTEX FLOW OF A DELTA WING WITH LEADING EDGE EXTENSION

Myong H. Sohn *
Korea Air Force Academy, ChungBuk-Do, Korea 363-849

Abstract

Effects of the existence of a centerbody on the vortex flow over a 65-deg delta wing with leading edge extension(LEX) was investigated experimentally through simultaneous off-surface visualization, wing-surface pressure and PIV measurements. The visualization and PIV measurements have captured all the essential and typical characteristics of the formation and interaction between both of the wing and LEX induced vortices. The qualitative investigation using these two techniques indicated that the effect of the centerbody existence on the vortex formation was found to be minimal at least at the experimental conditions from which the data was collected. However, the quantitative analysis of the wing-surface pressure measurements revealed the effects of centerbody existence to be prominent for the cases with the higher angles of attack and sideslip angles. Up to 24° angle of attack, the existence of the centerbody has a little influence on the suction pressure distribution of the upper wing surface of the present study even at the large sideslip angle of -20°. For the test cases with higher angles of attack of 28° and 32°, the existence of the centerbody caused a decrease in the magnitude of suction pressure distributions on both of the windward and leeward sides, and the difference of the suction pressure distribution between the two configurations increased as the magnitude of sideslip angle increased.

*Professor, Department of Aerospace Engineering(myongsohn@hanmail.net)

1 Introduction

The centerbody or fuselage-like structure of delta-wing-body geometries, which are used to meet the experimental needs or simulate the fuselage of real aircraft configurations, is known to affect significantly the delta-wing vortex flow. However, the complicated and multifaceted influence of the geometry of the centerbody or fuselage-like structure on the vortex dynamics of the delta-wing configuration is still controversial. For example, there exist contradicting results for the effect of centerbody on the vortex breakdown position of delta wings. Hanff and Jenkins[1] found that the vortex breakdown position of the 65-deg delta-wing-body configuration occurred significantly aft of the location measured by others for a pure 65-deg delta wing. The body configuration of Hanff and Jenkins' study was the pointed ogive for front-body whose tip was positioned behind the wing apex, and circular cylinder for aft-body. Hwang[2] investigated vortex dynamics of military-aircraft-configuration delta-wings of various sweep angles and centerbody configurations. He reported that there was no global effect of centerbody on the wing-surface pressure distribution.

However, Guglieri and Quagliotti[3] observed the presence of the fuselage-like structure under the lower surface of the delta wing promoted the position of vortex breakdown to move upstream as much as 20% chord for the sharp-edged 65-deg delta wing. Straka and Hemsch[4] also found that the adding a centerbody to the delta wing planform dramatically promoted the onset and chordwise progression of vortex breakdown(8-deg lower angle of attack with fuselage than

without fuselage). The experimental model of Straka and Hemsch's study was the flat-plate delta wing attached by the fuselage of pointed tangent-ogive front-body and 1.5 inch-diameter cylindrical aft-body. The big difference between Hanff and Jenkins' study and Straka and Hemsch's sudy was that the pointed body apex of Straka and Hemsch's model was ahead of the wing apex.

Ericsson[5, 6, 7] presented analysis for the flow physics associated with body-induced camber effect, and concluded that a centerbody or a fuselage of the delta-wing-body configuration have a profound effect on the vortex breakdown characteristics. He suggested that the pointed ogive centerbody ahead of the wing apex of Straka and Hemsch's study induced upwash along the leading edge and generated a negative camber effect which would result in promotion of the vortex breakdown. And the pointed ogival portion of the centerbody of Hanff and Jenkins' study where the pointed ogival portion of the centerbody was not located forward of the wing apex generated a positive wing-camber effect and resulted in delay of the vortex breakdown. Lowson and Riley[8] examined the reason of the wide variation of vortex breakdown position on delta wings at nominally identical angles of attack and sweep. They concluded that Reynolds number, strut position and visualization methods had little effect on vortex breakdown position, but the detail differences in geometry between the various experiments(such as wing thickness, leading-edge chamfers, reading-edge radius) made the wide variation of the vortex breakdown position. They argued that the apex shape was the key effect in determining the vortex breakdown position because the vorticity shed from the apex formed the center of the vortex core.

Most of previous research for the influences of fuselage geometry on delta-wing aerodynamics was focused on the vortex breakdown characteristics. Also effort of investigating flow phenomena and aerodynamic load characteristics simultaneously is few. Sohn and Lee[9, 10, 11] presented in great detail the results of wind tunnel tests of a 65-deg delta wing alone and with a uniquely shaped leading edge extension. They provided extensive upper-wing surface pressure data, off-surface visualization and flow field measurements of the wing leeward region through 5-hole probe and hot-film measurement for various angle of attack and sideslip angles. However, the pressure and flow field measurements were performed with the configuration with the centerbody under the lower wing surface, and the off-surface visualization was done with the configuration of reduced size and without centerbody. Also the effect of the centerbody was not considered seriously. It was thought that if an experimental study of assessing the effects of the difference between the two experimental models performed, the extensive flow physics and aerodynamic data of references 9, 10, and 11 would be more valuable.

The present study examines the vortex flow over a sharp-edged 65-deg delta wing with leading edge extension through simultaneous off-surface visualization and PIV measurement of the wing leeward flow region, and the wing-surface pressure measurement. The present study investigates the effect of the centerbody under the lower wing surface for various angles of attack and sideslip angles. It was tried to relate the measured aerodynamic load characteristics to the associated flow physics. Angles of attack of 20, 24, 28 and 32 degs were tested at the sideslip angles of 0, -5, -10, and –20 degs. Flow Reynolds numbers were 1.82×10^5 for the off-surface visualization and 1.76×10^6 for the wing-surface pressure measurement.

2 Experimental Procedure

2.1 Wind tunnel

The experimental apparatus was set up at the Korea Air Force Academy Subsonic Wind Tunnel. The medium-scale test facility is a closed-circuit atmospheric tunnel having test section 2.45m high and 3.5m wide. The maximum velocity is 92m/sec. The contraction ratio of the test section is 7.26:1 and the flow angularity is less than 0.1 deg. The axial

turbulence intensity(u'/U) of 0.04% at the free stream velocity of 74m/sec.

2.2 Test model

The experimental model used in the present study is the same one as in references 9 and 10. Figure 1 shows the geometry and picture of experimental model used in the present study.
The model has a flat wing with sharp leading edge of 65-deg sweep angle. The sharp leading edge was obtained by beveling 25 deg on the

lower surface, leaving the upper surface flat. The trailing edge was also beveled in the same way. The model has the root chord of 795 mm with the strake and the trailing edge has a span of 475.4 mm. The thickness of the wing section is 15 mm. The LEX is also a flat plate, 6.35 mm thick, and has symmetrically beveled leading and side edges. The planform of the LEX has the sweep angles of 65 and 90 degs. The lower wing surface is mounted with a centerbody that serves as the housing for the pressure tubes and the model support.
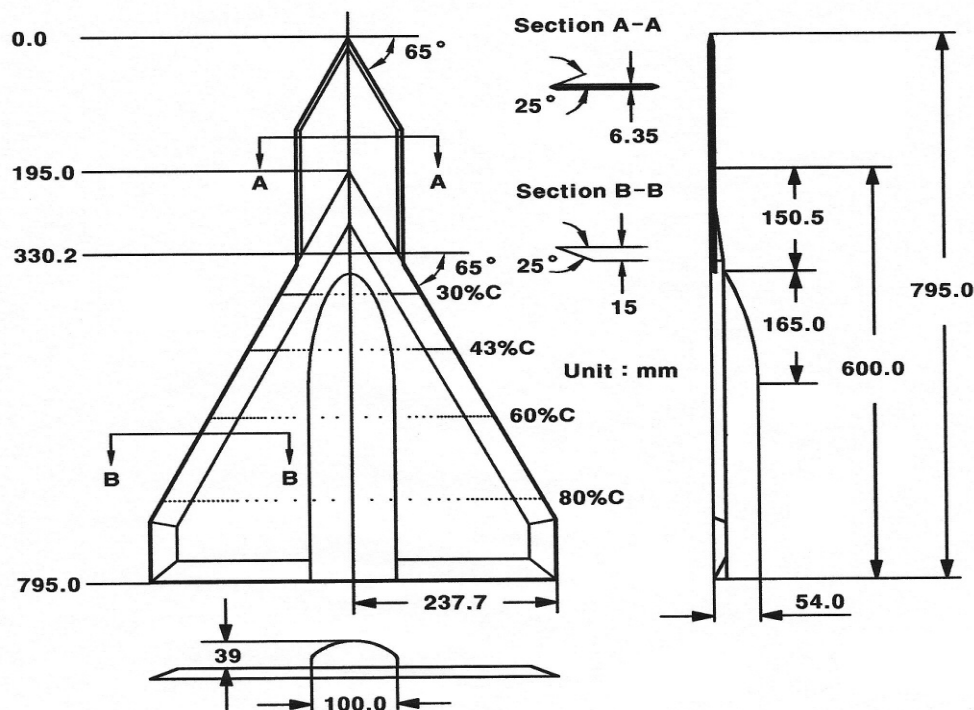
a) Geometry of model (Centerbody-on)

b) Photo of model (Centerbody-on)

Fig. 1. Model geometry and photographs

The centerbody of the present study is basically a rounded rectangular beam with an ogived apex as shown in Fig. 1(a). The width is 100 mm and the height is 39 mm. The ogived apex portion has the fineness ratio 4.23, and started 150.5 mm behind the main wing apex. The rear portion of the centerbody was attached to the support sting of diameter 50 mm and length 365 mm.

The wing was equipped with four spanwise rows of upper-surface static pressure taps on the whole wing. The pressure rows were located at the 30%, 43%, 60%, and 80% wing chord(c) stations, measured from the main wing apex. There were 47 pressure taps on each chord station along the entire span. The pressure taps on each chord station were located at the same relative span position normalized by a local semi-span, s. The nearest pressure tap to the wing's leading edge was located at the 0.025s point from the sharp leading edge. The accuracy of the model geometry was ascertained by almost perfect symmetric pressure distribution at zero sideslip.

The x direction is defined as the coordinate along the wing centerline, measured from the wing apex, y as the coordinate along the wing local semi-span measured from the wing centerline to the starboard side wing, and z as the coordinate normal to the upper wing surface.

2.3 Off-surface visualization

An off-surface flow visualization method using micro water droplets and a laser beam sheet was developed in the present study. Water droplets of 5-10 μm size were generated from a home-style ultrasonic humidifier. The water droplets exited just below the model apex and followed with the air stream without any external power. A 3 W Argon ion laser was used to generate the light sheet. The laser light sheet made by the cylindrical lens and the convex-focusing lens was used to interrogate specific cross sections of the wing leeward flow region. The laser light sheet was perpendicular to the upper wing surface and the wing centerline. The illuminated planes were

recorded by a high-resolution digital camera(SONY DCR-VX 2000 NTSC) which could take 30 frames per second. The camera was positioned at 1.658 m behind the trailing edge of the experimental model, and the line of sight of the camera was parallel to the upper wing surface. The laser light sheet on the traverse platform was moved downstream at a constant speed while the camera was taking pictures at a shutter speed of 1/90 sec.

For each flow condition, total frames of 460~480 were obtained while the laser light sheet was traveling from x/c=0.30 to 1.0. The flow visualization was carried out in the low-speed wind tunnel at the Korean Air Force Academy which had a test section 0.9 m high, 0.9 m wide, and 2 m long. The turbulence intensity was less than 0.2% for the available test section speed range from 3.6 m/s to 50 m/s. The flow Reynolds number was 1.82×10^5 based on the free stream velocity of 6.2 m/s and the main-wing root chord 400 mm. The details of the off-surface visualization is described in reference 11.

2.4 PIV measurement system

PIV System used in this study consists of a double-pulse Nd:YAG laser(Vlite-200) with maximum pulse energy of 200 mJ at a repetition rate of 10Hz, a 8-bit digital CCD with 2048×2048 pixels, and a PC equipped with DaVis FlowMaster software and a synchronization board developed by LaVision GmbH for the system synchronization, control, data acquisition and post-processing. Aerosol Generator was used for the seeding of DEHS($C_6H_{50}O_4$) particles. The mean diameter of the seeding particle was 1μm, and the density was $0.91 g/cm^3$.The particles were filled in the tunnel beforehand and the generator was turned off during the actual measurements. The schematic view of the experiments set-up is shown in Figure 2. The capture rate was 7 frames per second, and the measurement was done for 3 seconds. The PIV data was used to extract the cross-flow plane velocity vector and vorticity distribution.
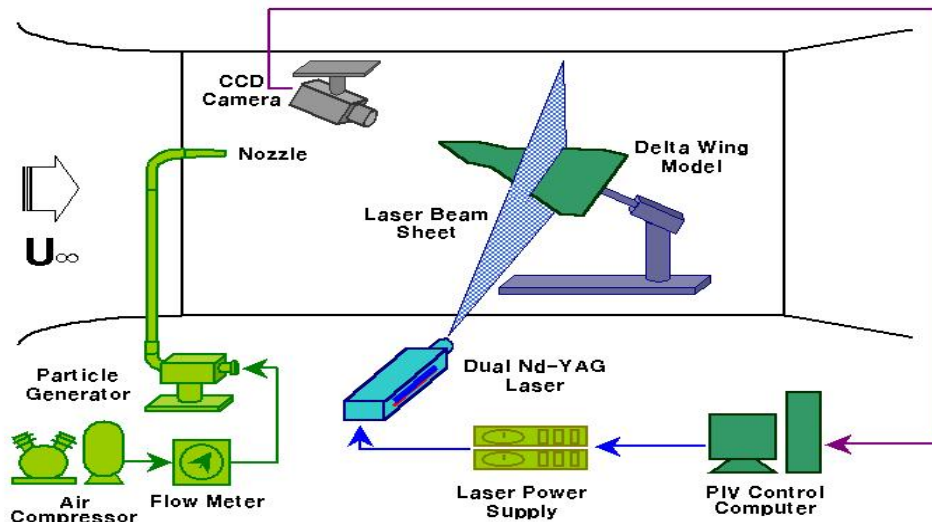
Fig. 2. Experimental set-up and PIV measurement system

2.5 Pressure measurement

The static pressure on the wing upper surface was measured by the PSI 8400 pressure measuring system. The measurement rate was 0.2 sec/measure. The wing surface pressure data in this study was an ensemble average of 300 pressure signals from each pressure tap. The measured pressure coefficient data was accurate within 3.2%. The flow Reynolds number was 1.76×10^6 based on the free stream velocity of 40 m/s and the main-wing root chord 600 mm.

3 Results and Discussions

3.1 Visualization results

Figure 3 compares the visualization section photos of leading-edge vortices at several chord stations with and without the centerbody. These section photos were selected from the dynamic images of video camera. The sideslip angle is zero, and the angle of attack is 28 deg. The upper photos show the cross-sectional view of the vortices for the configuration without centerbody and the lower ones show the cross-sectional view of the vortices for the configuration with centerbody.

The results show that the overall flow patterns such as the relative size and location of the vortices and their coiling interactions are very close to each other. At x/c=0.30(Fig. 3a), distinct LEX vortices exist in the wing leeward region, and wing vortices just started to develop in the vicinity of the wing leading edge. When going downstream, the wing vortex increased in strength and size. The wing and LEX vortices on each side of the wing co-rotated and migrated in the spanwise and normal directions according to the rule of mutual induction of a vortex pair with the same sense of rotation. The clockwise coiling of the wing and LEX vortices on the port side of the wing and the counterclockwise coiling of the wing and LEX vortices on the starboard side of the wing, continued when flowing downstream. The last frames of Fig. 3 show that the wing and LEX vortices merge to make a single vortex without breakdown at the trailing edge. A closer examination reveals that the existence of the centerbody accelerated coiling motion between the wing and LEX vortices.

The analysis of the dynamics images of a cross-section at a specific chord position showed the unsteadiness of the coiling state of the wing and LEX vortices, and this resulted in

5
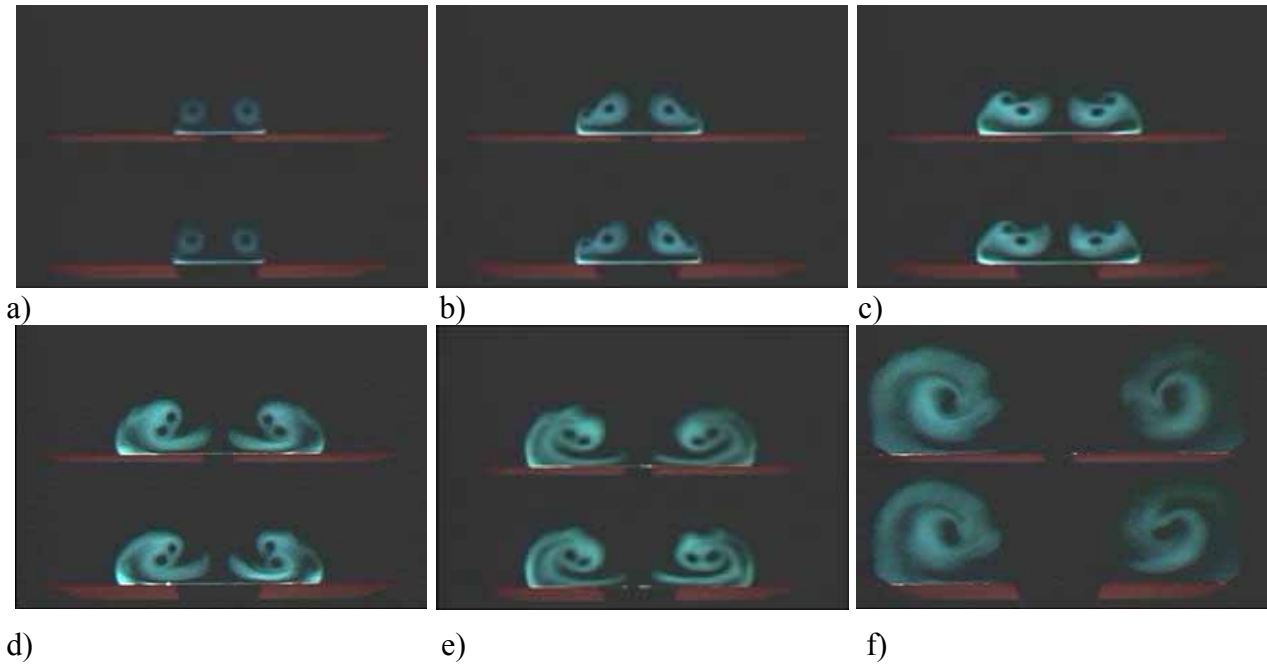
Fig. 3. Comparison of visualization results for CB-off(upper photo) and on(lower photo) configurations (α=28 deg, β =0 deg): a) x/c=0.30; b) x/c=0.40; c) x/c=0.50; d) x/c=0.60; e) x/c=0.70; f) x/c=1.0

the wandering of the core positions of the wing and LEX vortices. This wandering was increased as traveling downstream at higher angles of attack. Even though this unsteadiness of the vortex system is considered, the advanced coiling of the wing and LEX vortices observed in Fig. 3 is characteristic of the centerbody-on configuration. The PIV measurement also convinces this argument, which will be shown later.

Figures 4, 5 and 6 compares the visualization results of the centerbody-off and on configurations at specific chord positions for the angle of attack, 24 deg. Two specific chord positions, x/c=0.43 and 0.60, were selected. The former represented upstream chord position and the latter downstream chord position. Figure 4 shows that at x/c=0.43 the vortex characteristics such as the relative positions of the wing and LEX vortices and their interaction is nearly identical both for the centerbody-off and on configurations, but at x/c=0.60 the coiling of the wing and LEX vortices is advanced for the centerbody-on configuration. The same

argument applies to the cases of the sideslip angles of –5 deg and –10 deg as shown in Figs. 5 and 6, even though the difference between the centerbody-off and on configurations is not distinct due to the overwhelming effect of sideslip angle.

The effect of sideslip angle is exhibited vividly in Figs. 5 and 6. At the 43% chord station, the coiling of the wing vortex and the LEX vortex was advanced slightly on the windward side, but the coiling of them was significantly delayed. As a consequence of different coiling state on the windward and leeward sides of the wing, the wing vortex and the LEX vortex positioned laterally along the wing surface on the windward side, but they move outboard and away from the wing surface on the leeward side. At the 60% chord station, the windward wing and LEX vortices coalesced and diffused, while the leeward wing and LEX vortices had distinct cores and floated away from the wing surface. The effect of sideslip overwhelms the effect of the centerbody. The change of the vortex flow due to the sideslip angle observed in Figs. 5 and 6 is consistent with other studies of vortex flows of yawed double-delta wings[11, 12].
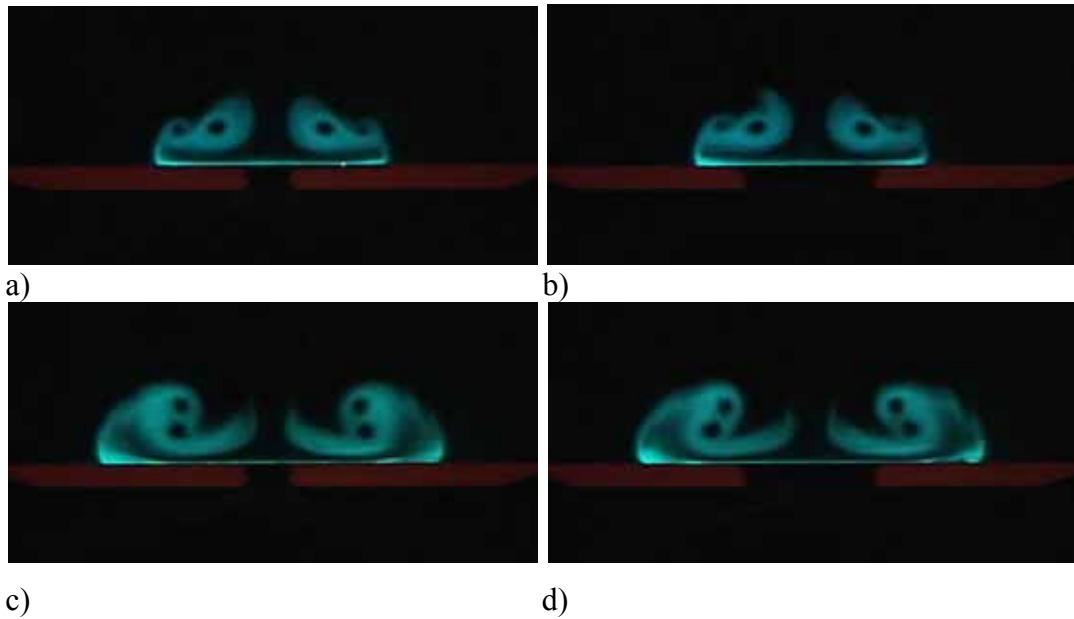
**Fig. 4. Comparison of visualization results for CB-off and on configurations
(α= 24 deg , β = 0 deg) : a) CB-off, x/c=0.43; b) CB-on, x/c=0.43; c) CB-off,
x/c=0.60; d) CB-on, x/c=0.60**
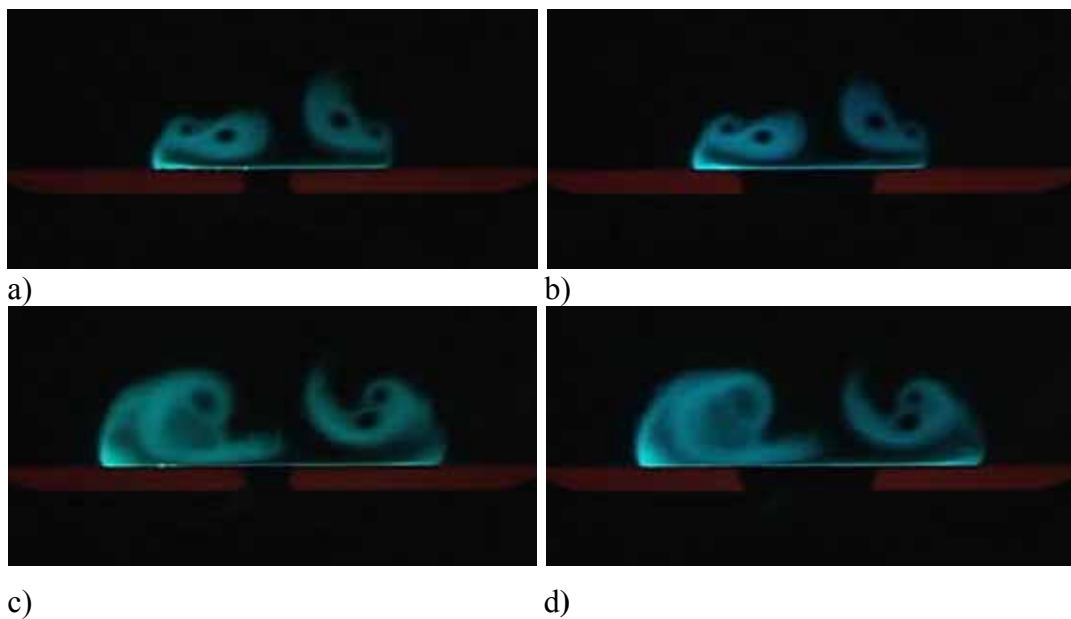
**Fig. 5. Comparison of visualization results for CB-off and on configurations
(α=24 deg, β = -5 deg) : a) CB-off, x/c=0.43; b) CB-on, x/c=0.43; c) CB-off,
x/c=0.60; d) CB-on, x/c=0.60**
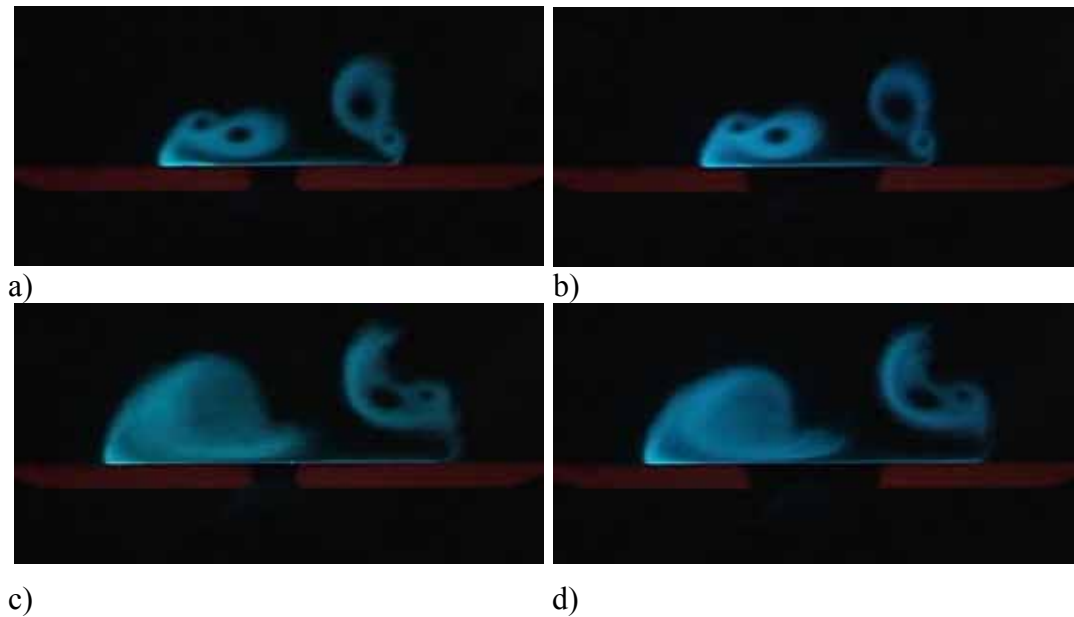
Fig. 6. Comparison of visualization results for CB-off and on configurations (α=24 deg, β = -10 deg) : a) CB-off, x/c=0.43; b) CB-on, x/c=0.43; c) CB-off, x/c=0.60; d) CB-on, x/c=0.60

3.2 PIV measurement and Reynolds number effect

In the present simultaneous off-surface visualization, PIV measurements, and wing-surface pressure measurement study for the delta-wing vortex flow, the free stream velocity and the model size for the off-surface visualization had to be reduced due to the limitation of the experimental facility. It is well known that the vortex flow of delta wings is not sensitive to the flow Reynolds number if the sharp leading edge is guaranteed. An experiment of assessing the effect of the Reynolds number was performed in order to properly relate the flow physics obtained form the visualization result to the wing-surface pressure distribution characteristics. PIV measurement can provide both qualitative flow pattern and quantitative information such as velocity field and vorticity field. The PIV measurements of the wing leeward region for the centerbody-on model was conducted for three different free stream velocities, 10, 20, and 40 m/sec. The flow Reynolds numbers based on the model-wing chord(600mm) and the three

different free stream velocities are, 0.44×10^6, 0.88×10^6, and 1.76×10^6, respectively.

Figure 7 compares the velocity field(cross flow velocity) and the vorticity field(streamwise vorticity) for the three different Reynolds numbers at the two representative chord positions, x/c=0.43 and x/c=0.60. At x/c=0.43(left column of Fig. 7) the difference of the Reynolds numbers did not affect the vortex characteristics such as the relative positions and scaled strengths of the wing and LEX vortices. The maximum values of the cross-flow velocity vectors were 14.9m/s, 30.2m/s, and 60.7m/s, respectively, for the three free stream velocities 10m/s, 20m/s, and 40m/s. Therefore, the ratios of the maximum cross flow velocities to the free stream velocities are 1.49, 1.51, and 1.52. The core positions(positions of maximum magnitude of vorticity) at upstream chord position x/c=0.43, are minimal at least for the sharp-edged delta wing with LEX of the present study.

However, the similarity of the vortex characteristics for different Reynolds numbers is not guaranteed at downstream chord position x/c=0.60. First, the symmetry of the vortex flows of the port-side wing-half and the
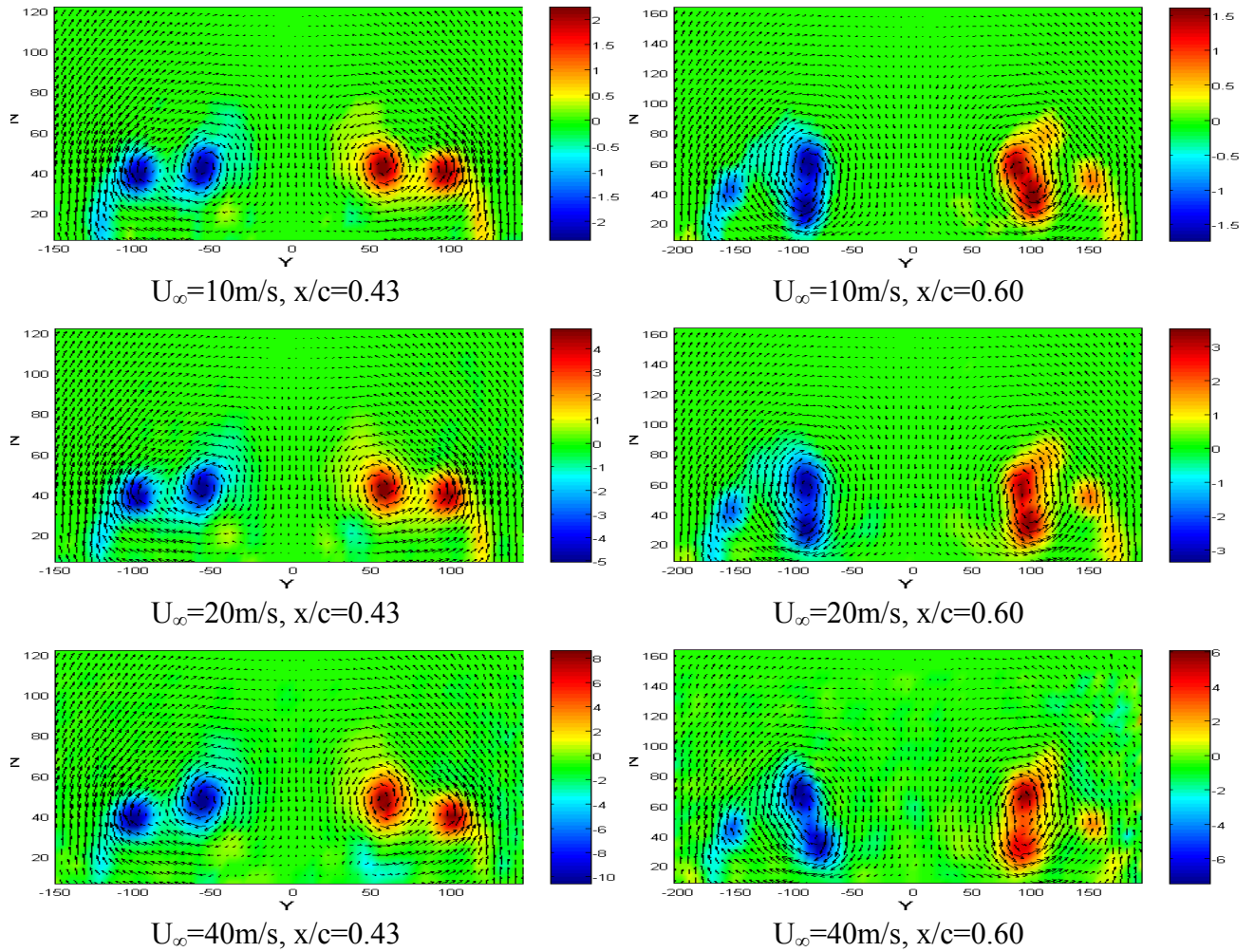
Fig. 7. Effect of Reynolds number on PIV-measured data (centerbody-on configuration, α=24 deg, β=0 deg)

starboard-side wing half is worsened at x/c=0.60. The coiling of the wing and LEX vortices is delayed on the port side of the wing and it is advanced on the starboard side of the wing. This asymmetry of the vortex system on the two sides of the wing at zero sideslip observed in Fig. 7 is somewhat disappointed. The decreased resolution of the PIV measurement and/or the intrinsic flow unsteadiness might cause the asymmetry of the flow at the 60% chord position. The second fact observed in the PIV data of Fig. 7 is that as Reynolds number is increased, the coiling of the wing and LEX vortices is delayed both on the port and starboard sides of the wing. Comparing the visualization result at the same angle of attack

and chord position(Fig. 4) with Fig. 7, it is noticed that the coiling angles of the wing and LEX vortices(defined as the angle between the reference line and the line connecting the cores of the wing and LEX vortices) of PIV data for all 3 different Reynolds numbers are slightly smaller than the coiling angle of the visualization result which was obtained at the Reynolds number of 1.82×10^5. The maximum values of the cross-flow velocity vectors at x/c=0.60 were 16.1 m/s, 32.6 m/s, and 58.5 m/s, respectively for the three free stream velocities 10 m/s, 20 m/s, and 40 m/s. Therefore, the ratios of the maximum cross flow velocities to the free stream velocities are 1.61, 1.63, and 1.46.

Figure 8 compares the velocity field and the

U_∞=10m/s, x/c=0.43 U_∞=10m/s, x/c=0.60

U_∞=20m/s, x/c=0.43 U_∞=20m/s, x/c=0.60

U_∞=40m/s, x/c=0.43 U_∞=40m/s, x/c=0.60
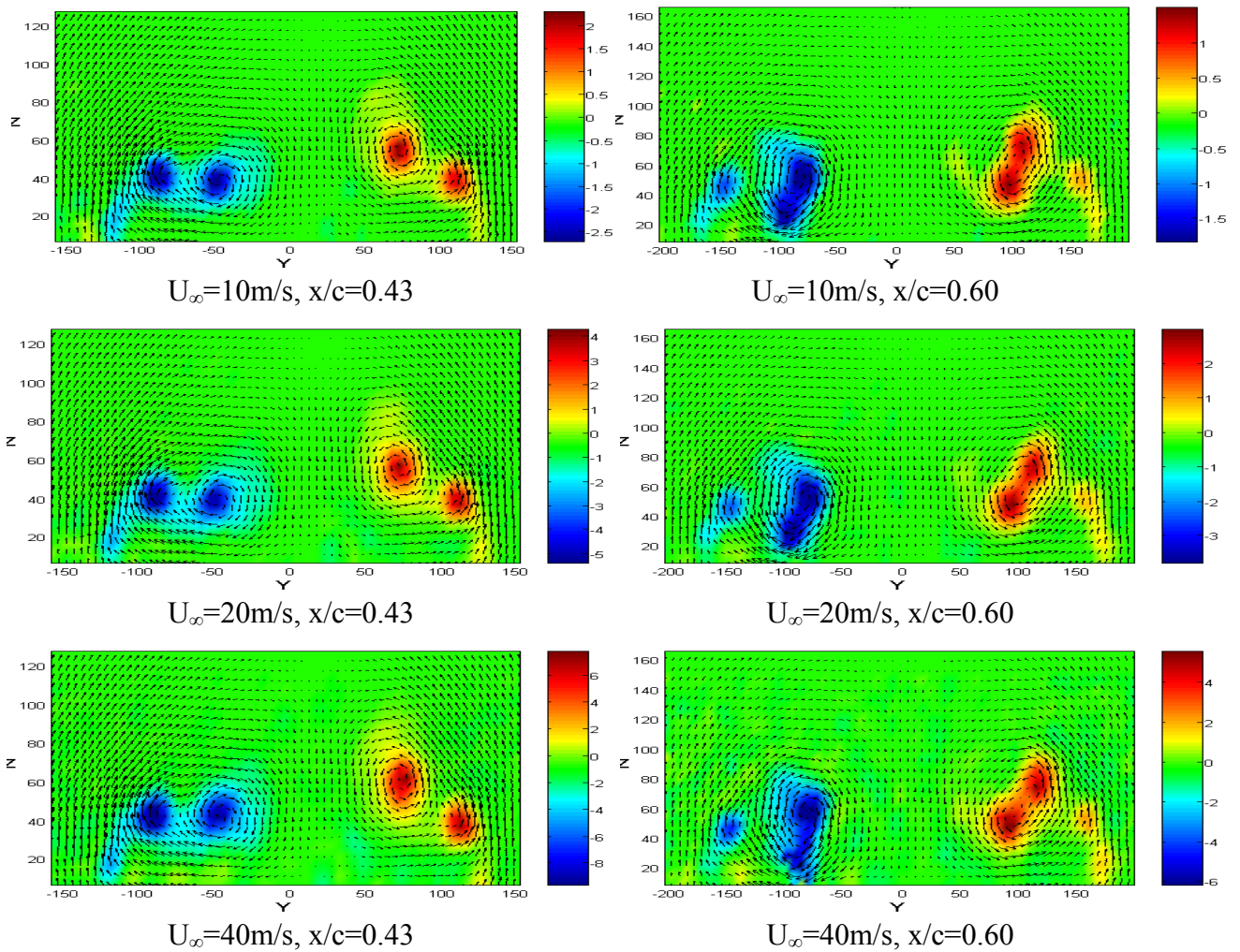
Fig. 8. Effect of Reynolds number on PIV-measured data (centerbody-on configuration, α=24 deg, β=-5 deg)

vorticity field for the three different Reynolds number for non-zero sideslip case. The angle of attack is 24 deg and the sideslip angle is −5 deg. The effect of sideslip represented by the increased coiling and closer-to-wing movement of the windward wing and LEX vortices and the decreased coiling and floating-away-from-wing movement of the leeward wing and LEX vortices, is well captured. The delayed coiling of the wing and LEX vortices at higher Reynolds number is also observed in Fig. 8, especially at the 60% chord position(right column of Fig. 8). The difference between the coiling angles of different Reynolds numbers at β= −5 deg is minor compared to the case of zero sideslip.

Even though more refined and extended investigation is needed for the definite conclusion, the effect of the Reynolds number for the sharp-edged delta wing with LEX of the present study can be summarized as follows. The effect of flow Reynolds number on the vortex flow of the sharp-edged delta wing with LEX of the present study is insignificant at upstream chord positions, but it resumes as traveling downstream. The effect of Reynolds number on the vortex flow was that at higher Reynolds number the coiling interaction of the wing and LEX vortices of same sense of rotation was delayed. This delayed coiling interaction was applied to both zero sideslip and non-zero sideslip with decreased influence of Reynolds number for the non-zero sideslip.

10

CB-off, x/c=0.43

CB-on, x/c=0.43

CB-off, x/c=0.60

CB-on, x/c=0.60
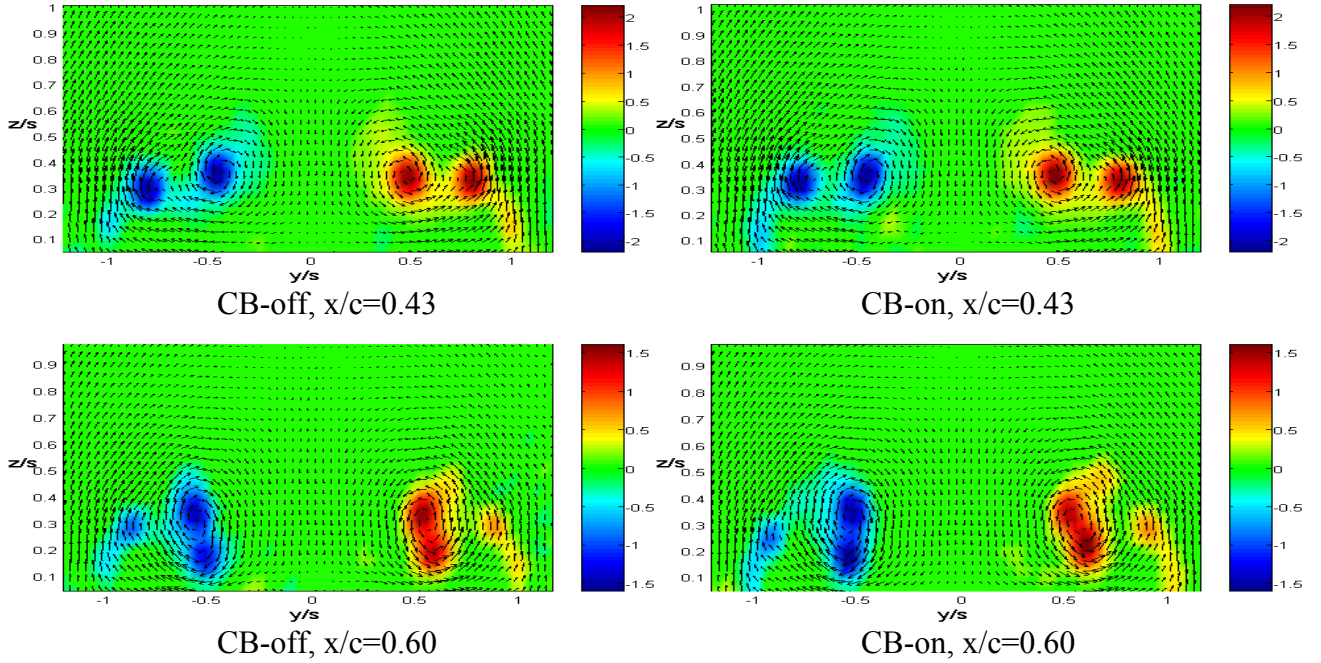
**Fig. 9. Comparison of PIV measurement for centerbody-off and on configurations
(V_∞=10m/s, α=24 deg, β=0 deg)**

Figures 9 compares the PIV measurements of the centerbody-off and on configurations at the two representative chord positions, x/c=0.43 and x/c=0.60. The angle of attack was 24 deg, and sideslip angles is zero. The results at the 43% station show a negligible difference between the two cases in terms of the relative locations of the vortices and their strength. The core positions(positions of maximum magnitude of vorticity) of the wing and LEX vortices are compared in Table 1. The value of streamwise vorticity was obtained by differentiating the cross flow velocity measured by PIV. At the 43% chord station of the centerbody-off configuration, the vorticity value of the LEX vortex core was -2.254 sec^{-1} and that of the wing vortex core was -2.215 sec^{-1} on the port side. The vorticity value of the LEX vortex core was 2.208 sec^{-1} and that of the wing vortex core was 2.227 sec^{-1} on the starboard side. At the 43% chord station of the centerbody-on configuration, the vorticity value of the LEX vortex core was -2.288 sec^{-1} and that of the wing vortex core was -2.370 sec^{-1} on the port side. The vorticity value of the LEX vortex core was 2.232 sec^{-1} and that of the wing vortex core was 2.208 sec^{-1} on the starboard side.

Table 1. Vortex core positions (α=24 deg, β=0 deg)

		port side		starboard side	
		wing	LEX	wing	LEX
x/c= 0.43	CB-off	y/s= -0.805 z/s= 0.305	y/s= -0.450 z/s= 0.364	y/s= 0.810 z/s= 0.345	y/s= 0.495 z/s= 0.364
	CB-on	y/s= -0.798 z/s= 0.352	y/s= -0.461 z/s= 0.372	y/s= 0.808 z/s= 0.352	y/s= 0.490 z/s= 0.372
x/c= 0.60	CB-off	y/s= -0.563 z/s= 0.311	y/s= -0.525 z/s= 0.158	y/s= 0.549 z/s= 0.350	y/s= 0.587 z/s= 0.196
	CB-on	y/s= -0.532 z/s= 0.355	y/s= -0.571 z/s= 0.163	y/s= 0.504 z/s= 0.355	y/s= 0.580 z/s= 0.201

The comparison shows that the difference of the vortex core positions and strengths between the two configurations at the 43% chord station is minimal at least for the sharp-edged delta

CB-off, x/c=0.43

CB-on, x/c=0.43

CB-off, x/c=0.60

CB-on, x/c=0.60
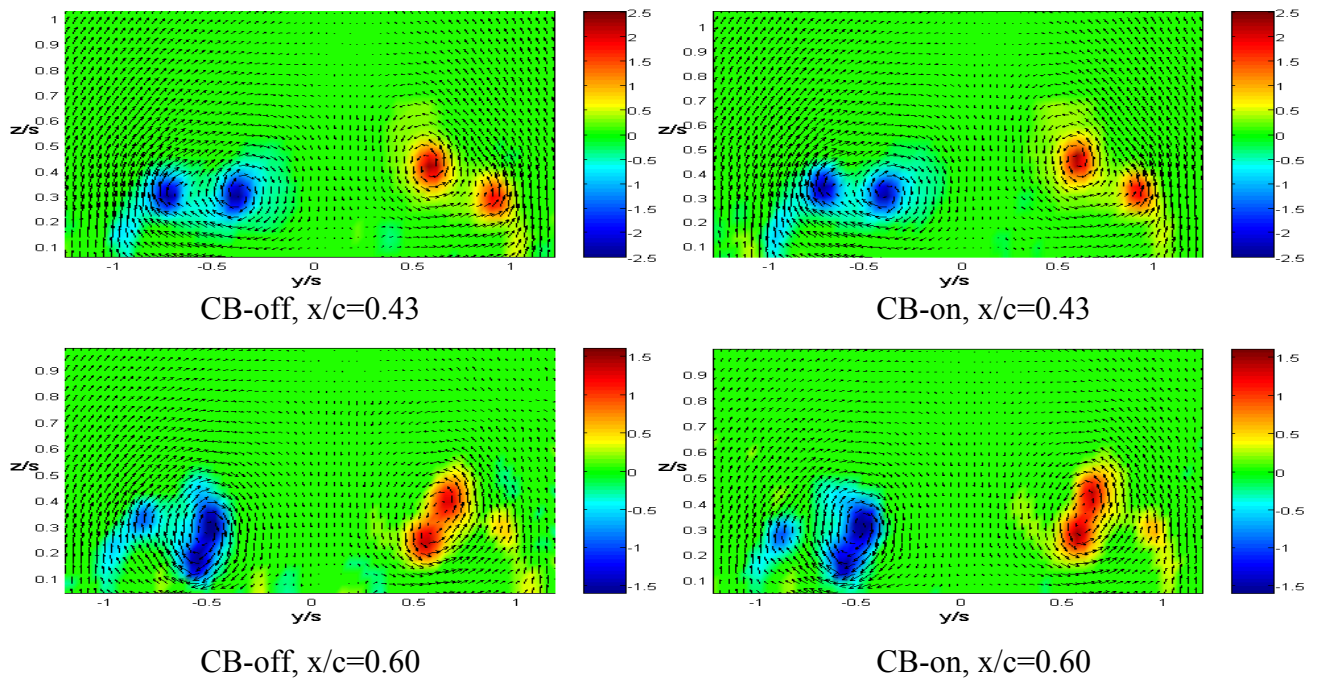
Fig. 10. Comparison of PIV measurement for centerbody-off and on configurations (V_∞=10m/s, α=24 deg, β=-5 deg)

wing with LEX of the present study.

This tendency generally continues to the 60% station location; however, the differences between the two cases become somewhat notable. As in the visualization study, the coiling motion between the two vortex systems is enhanced for the centerbody-on case. The symmetry of the vortex flows of the port-side wing-half and the starboard-side wing half is worsened at x/c=0.60 both for the centerbody-off and on configurations. This asymmetry in the PIV measurement at x/c=0.60 is relatively large compared to the visualization results at the same chord position.

Figure 10 compares the PIV measurements of the centerbody-off and on configurations at the non-zero sideslip angle. The sideslip angle is –5 deg. The chord positions, angle of attack, and the free stream velocity were same as in Fig. 9. Figure 10 shows that the same argument can be said for the case of –5 deg sideslip angle. The relative locations of the vortices and their strengths for the two configurations showed negligible difference at the 43% chord station. At the 60% chord station, coiling of the wing

and LEX vortices for the centerbody-on configuration is slightly advanced than the centerbody-off configuration. The core positions of the vortices are compared in Table 2.

Table 2. Vortex core positions (α=24 deg, β=-5 deg)

		port side		starboard side	
		wing	LEX	wing	LEX
x/c= 0.43	CB-off	y/s= -0.745 z/s= 0.297	y/s= -0.385 z/s= 0.297	y/s= 0.895 z/s= 0.297	y/s= 0.575 z/s= 0.417
	CB-on	y/s= -0.737 z/s= 0.345	y/s= -0.405 z/s= 0.304	y/s= 0.924 z/s= 0.304	y/s= 0.592 z/s= 0.470
x/c= 0.60	CB-off	y/s= -0.516 z/s= 0.314	y/s= -0.555 z/s= 0.178	y/s= 0.642 z/s= 0.391	y/s= 0.565 z/s= 0.237
	CB-on	y/s= -0.488 z/s= 0.322	y/s= -0.566 z/s= 0.166	y/s= 0.644 z/s= 0.439	y/s= 0.566 z/s= 0.283

**Fig. 11. Comparison of wing-surface pressure distributions at different chord positions
and angles of attack for zero sideslip angle (open symbols; CB-off, solid symbols; CB-on):
a) x/c =0.30, b)x/c=0.43, c) x/c=0.60, d) x/c=0.80**

Figure 10 and Table 2 also shows the effect of sideslip. The strengths of the LEX and wing vortices were increased on the windward side, but those were decreased on the leeward side, compared to zero sideslip. For example, the vorticity value of the LEX vortex core was -2.416 sec^{-1} and that of the wing vortex core was -2.706 sec^{-1} on the windward side for the 43% chord station of the centerbody-on configuration. However, the vorticity value of the LEX vortex core was 2.293 sec^{-1} and that of the wing vortex core was 1.838 sec^{-1} on the leeward side for the same chord station and the same configuration.

3.3 Wing-surface pressure distribution

Figure 11 compares the upper-wing-surface pressure distributions of the centerbody-off and on configurations at several angles of attack and zero sideslip angle. The open symbols denote the centerbody-off configuration and the solid symbol denote the centerbody-on configuration. It shows that the difference of suction pressure distribution between the two configurations is minor for all angles of attack tested. Also a good symmetry for the pressure distributions on the port side and starboard side of the wing is observed for all angles of attack and chord stations. The almost perfect symmetric pressure distribution at zero sideslip angle shown in Fig. 11 demonstrates that the present study excludes model imperfections and asymmetric free stream flow conditions, which might cause asymmetric vortex development and breakdown even at zero sideslip. The centerbody-off configuration has slightly larger magnitude of suction pressure than the centerbody-on configuration, but the difference is considered to

13
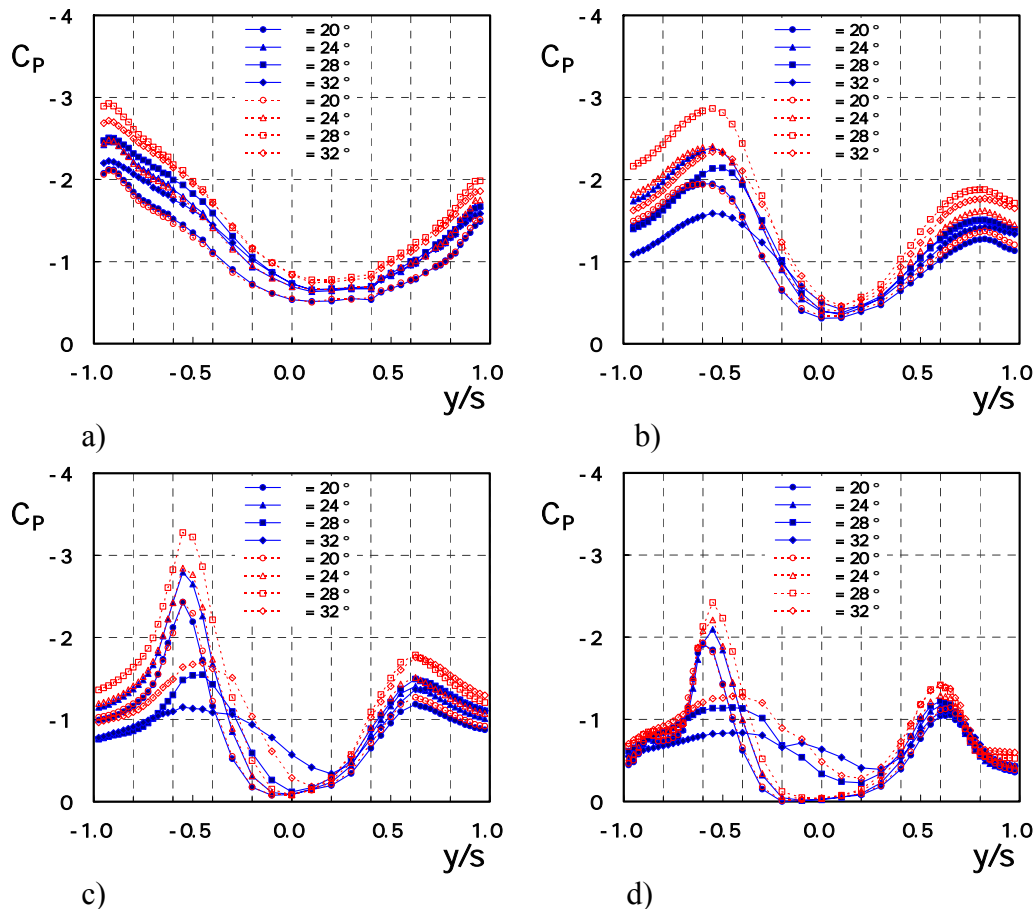
Fig. 12. Comparison of wing-surface pressure distributions at different chord positions and angles of attack for –5 deg sideslip angle (open symbols; CB-off, solid symbols; CB-on): a) x/c =0.30, b) x/c=0.43, c) x/c=0.60, d) x/c=0.80

be within the error of pressure measurement.

The suction pressure on the wing-upper surface is the footprint of the strengths and the relative positions of the vortices existing in the wing-leeward wake region. Comparing the visualization result of Fig. 3 with the upper-wing surface pressure distribution of Fig. 11, this argument is easily corroborated. At the 30% chord station the highest suction pressure peak occurs near the wing leading edge. The concentrated wing vortex adjacent to the wing leading edge observed in Fig. 3(a) causes this highest suction pressure at the 30% chord station. At the 43% chord station the wing vortex and the LEX vortex are located laterally with nearly the same vertical distance from the wing surface, which causes a single rounded suction-pressure peak. At the 60% chord station

the wing vortex and the LEX vortex are positioned almost vertically. With this relative position of the wing vortex and the LEX vortex, a single suction-pressure peak with a steep gradient was evident. The single suction-pressure peak of reduced magnitude at the 80% chord station is the reflection of the merging and diffusion of the wing and LEX vortices.

Figure 12 compares the upper-wing-surface pressure distributions of the centerbody-off and on configurations at sideslip angle of –5 deg. It is observed that the difference of the suction pressure distribution between the two configurations is no longer negligible for the non-zero sideslip angle. The centerbody-off configuration has the larger magnitude of suction pressure than the centerbody-on configuration at all angles of attack and at all chord stations. At higher angles of attack(28 and

14
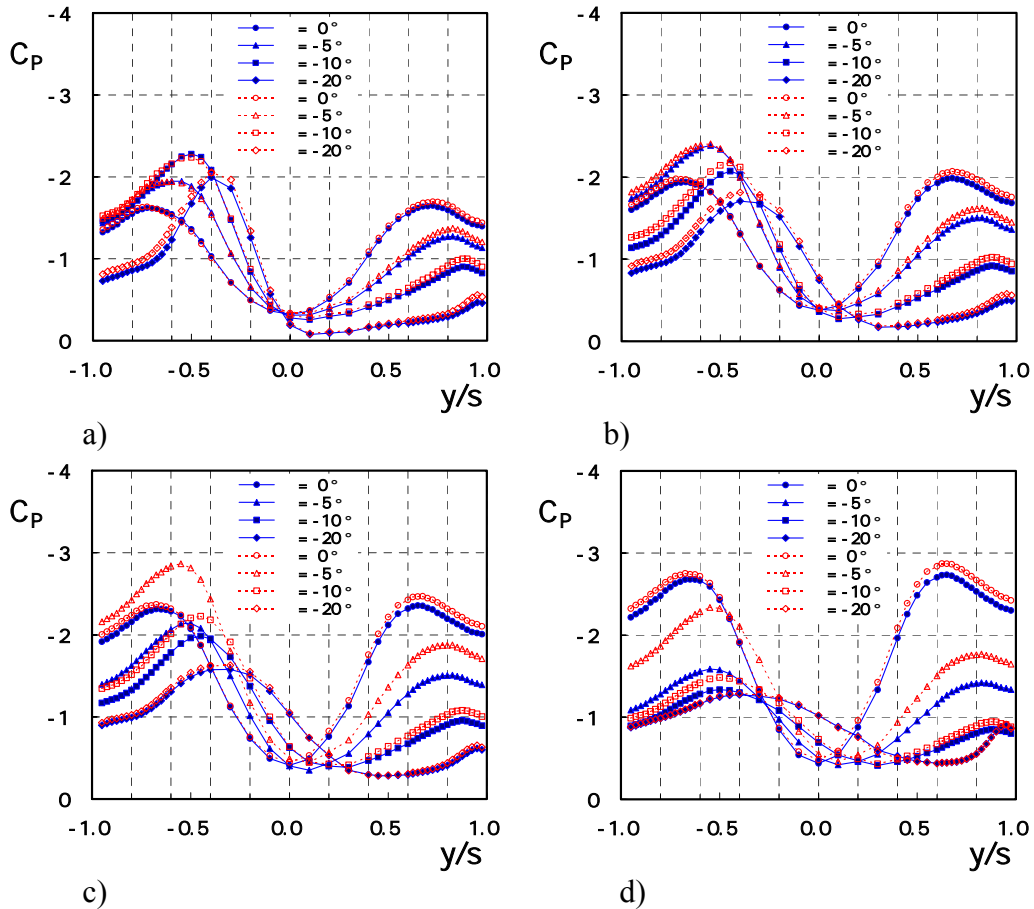
**Fig. 13. Comparison of wing-surface pressure distributions at different angles of attack
and sidelslip angles for x/c=0.43 (open symbols; CB-off, solid symbols; CB-on): a) α=20
deg, b) α=24 deg, c) α=28 deg, d) α=32 deg**

32 degs), the windward suction pressure distribution of the centerbody-on configuration show earlier diffusion and collapse than the centerbody-off configuration. For example, the windward suction pressure of the centerbody-off configuration remains high up to α=28 deg both at x/c=0.60 and 0.80, but that of the centerbody-on configuration at α=28 deg is reduced significantly at x/c=0.60 and completely collapsed at x/c=0.80.

Figure 13 shows the effect of sideslip and angle of attack on the wing-surface pressure distributions of the configurations with and without centerbody at the 43% chord station. At the angles of attack, 20 and 24 degs(Figs. 13(a) and (b)), the difference between the suction pressure distributions of two configurations is not significant for all sideslip angles tested. However, at the higher angles of attack, 28 and

32 degs(Fig. 13(c) and (d)), the pressure distributions of the two configurations start to show recognizable differences. The centerbody-on configuration has the smaller magnitude of suction pressure than the centerbody-off configuration for all 4 sideslip angles both on the windward and leeward sides. The difference of pressure distribution between the two configurations is largest for the sideslip angle of –5 deg. For the sideslip angles of larger magnitude, -10 and –20 degs, the difference of pressure distribution between the two configurations is rather small due to the reduced magnitude of suction pressure at the higher angles of attack.

In summary, up to 24 deg angle of attack, the existence of the centerbody had a little influence on the suction pressure distribution of the upper wing surface of the sharp-edged delta wing with LEX of the present study even at the quite large

15

sideslip angles(-10 and –20 degs). At the higher angles of attack of 28 and 32 degs, the centerbody-on configuration showed suction pressure distribution of decreased magnitude both upstream and downstream chord stations and earlier collapse at downstream chord stations at non-zero sideslip angle. The difference of the suction pressure distribution between the two configurations increased as the magnitude of sideslip angle increased.

4 Conclusion

Effects of the existence of a centerbody on the vortex flow over a 65-deg delta wing with leading edge extension(LEX) was experimentally investigated through simultaneous off-surface visualization, wing-surface pressure and PIV measurements. It was attempted to relate the observed flow physics to the characteristics of the measured aerodynamic load. With the extensive analysis of the experimental data obtained from the wind tunnel testing, the following conclusions were reached :

(1) The visualization and PIV measurements have captured all the essential and typical characteristics of the formation and interaction between both of the wing and strake induced vortices. The qualitative comparison of the results obtained from the two methods showed a very good agreement validating the accuracies of both techniques.

(2) The qualitative investigation using these two techniques indicated that the effect of the centerbody existence on the vortex formation was found to be minimal at least at the experimental conditions from which the data was collected(α=24 deg, β=0 and -5 degs). However, the quantitative analysis of the pressure measurements revealed the effects of centerbody existence to be prominent for the cases with the higher angles of attack and sideslip angles.

(3) Up to 24 deg angle of attack, the existence of the centerbody has a little influence on the suction pressure distribution of the upper wing surface of the sharp-edged delta wing with LEX used in the present study even at the large sideslip angle of -20 deg.

(4) For the test cases with higher angles of attack of 28 and 32 degs, the existence of the centerbody caused a decrease in the magnitude of suction pressure distributions on both of the windward and leeward sides, and the difference of the suction pressure distribution between the two configurations increased as the magnitude of sideslip angle increased.

References

[1] Hanff, E. S., and Jenkins, S. B., "Large-Amplitude High Rate Roll Experiments on a Delta and Double-Delta Wing," *AIAA Paper* 90-0224, January 1990.

[2] Huang, X. Z., "Comprehensive Experimental Studies on Vortex Dynamics over Military Wing Configurations in IAR," *AIAA Paper* 2003-3940, June 2003.

[3] Guglieri, G., and Quagliotti, F. B., "Experimental Investigation of Vortex Dynamics on a 65 Delta Wing," *AIAA Paper* 92-2731, June 1992.

[4] Straka, W. A., and Hemsch, M. J., "Effect of a Fuselage on Delta Wing Vortex Breakdown," *Journal of Aircraft,* Vol. 31, No. 4, 1994, pp. 1002-1005.

[5] Ericsson, L. E. and Beyers, M. E., "Ground Facility interference Effects on Slender Vehicle Unsteady Aerodynamics," *Journal of Aircraft,* Vol. 33, No. 16, 1996, pp. 117-124.

[6] Ericsson, L. E., "Effect of Fuselage Geometry on Delta-Wing Vortex Breakdown," *Journal of Aircraft,* Vol. 35, No. 6, 1998, pp. 898-904.

[7] Ericsson, L. E., "Multifaceted Influence of Fuselage geometry on Delta-Wing Aerodynamics," *Journal of Aircraft,* Vol. 40, No. 1, 2003, pp. 204-206.

[8] Lownson, M. V. and Riley, A. J., "Vortex Breakdown Control by Delta Wing Geometry," *Journal of Aircraft,* Vol. 32, No. 4, 1995, pp. 832-838.

[9] Sohn, M. H., and Lee, K. Y., "Experimental Investigation of a Yawed Delta Wing Having Leading Edge Extension," *AIAA Paper* 2002-3267, June 2002.

[10] Sohn, M. H. and Lee, K. Y., "Effects of Sideslip on the High-Incidence Vortical Flow of a Delta Wing with the Leading Edge Extension," *AIAA Paper* 2003-1107, January 2003.

[11] Sohn, M. H., Lee, K. Y., and Chang, J. W., "Vortex Flow Visualization of a Yawed Delta Wing with Leading-Edge Extension," *Journal of Aircraft,* Vol. 41, No. 2, 2004, pp. 231-237.

[12] Grismer, D. S., and Nelson, R. C., "Double-Delta-Wing Aerodynamics for Pitching Motions With and Without Sideslip," Journal of Aircraft, Vol. 32, No. 6, 1995, pp. 1303-1311.